Micro-needle patch based on dissolving, detachable micro-needle technology for improved skin quality. Part 1: Ex-Vivo Safety Evaluation

Authors: V. Zvezdin[§], L. Peno-Mazzarino**, N. Radionov**, T.Kasatkina*, I. Kasatkin*

§ Microneedles Inc., Delaware, USA

*Microneedle Industrial LLC, Moscow, Russia

**Laboratoire BIO-EC, Chemin de Saulxier 1, 91160 Longjumeau, France

Running header: Histological evaluation of microneedle patches

Correspondence: Laurent Peno-Mazzarino, Technical Director

Phone: (+33)1 69 41 47 61

Email: l.peno-mazzarino@bio-ec.fr

Email address of all authors:

V. Zvezdin - zvedin_v@mnlab.ru

T.Kasatkina - tania.akafeva@gmail.com

I. Kasatkin – ivankasatkin91@gmail.com

L.Peno-Mazzarino - l.peno-mazzarino@bio-ec.fr

N. Radionov - n.radionov@bio-ec.fr

This article has been accepted for publication and undergone full peer review but has not been through the copyediting, typesetting, pagination and proofreading process, which may lead to differences between this version and the Version of Record. Please cite this article as doi: 10.1111/ICS.12627

Key Words: skin explants, micro-needle patch, hyaluronic acid, ferulic acid, FITC, cell viability

Abstract:

OBJECTIVE: The aim of the paper presented herein is the description and safety evaluation of the process of dissolution of an 86 micro-needle patch composed of hyaluronic acid, when applied topically to human abdominal skin explants. Such explants were chosen to replace the inability of obtaining periorbital skin. In order to evaluate penetration and dissolution of the micro-needles we employed histochemical methods and a fluorescent dye FITC (fluorescein isothiocyanate).

METHODS: Abdominoplasty human skin explants were treated with square microneedle patches with a 1,5 cm^2 surface area, containing 86 micro-needles and having 450±23,5 µm in height with 1 mm interspacing between nearest neighbouring micro-needles. Histological processing and staining for cell viability, FITC distributions and glycosaminoglycans was performed. The stained surface percentage for each treatment was compared to control untreated samples at given time points. A Mann-Whitney Test was used to identify the difference between two populations (sites of skin samples punctured with stained and clear micro-needles respectively) at the given level of statistical significance ($p<0.05$).

RESULTS: The application of the MN patch to excised skin explants showed these micro-needles to be non-invasive into the dermis of the skin. Skin puncturing with MN patches revealed 17 different sites of micro-needle penetration immediately afterwards and 4 sites, 2 hours later. While there were some variances in the epidermal depth of penetration, these variances did not impact on cell viability. The hyaluronic acid-based micro-needles having 450 µm in length penetrated the epidermis at an averaged depth by 26 µm without disrupting skin cell viability and without causing an inflammatory response. Hyaluronic acid could be detected in most of these penetration sites, with no diffusion into the dermis., which is important for cosmetic applications. FTIC analysis uncovered fluorescein isothiocyanate distribution within micro-needle insertion site which remained steady after 2 and 6 hours of experimentation.

CONCLUSIONS: Using ex-vivo tracer staining studies, we have shown that the evaluated micro-needle applicator is capable of penetrating the skins epidermis and deliver substances embedded in the needle polymer matrix. In addition, the tested product was shown to be safe, which provides for a broad perspective for delivering cosmetic and pharmaceutic agents.

Resumé:

OBJECTIF: Le but de cet article est de décrire et évaluer l'innocuité du processus de dissolution d'un patch de 86 micro-aiguilles composé d'acide hyaluronique, lorsqu'il est appliqué par voie topique sur des explants de peau abdominale humaine. De tels explants ont été choisis pour palier à

l'impossibilité d'obtenir une peau périorbitaire. Afin d'évaluer la pénétration et la dissolution des micro-aiguilles, nous avons utilisé des méthodes histochimiques et un marqueur fluorescent FITC (isothiocyanate de fluorescéine).

MÉTHODES: Les explants de la peau humaine de l'abdominoplastie ont été traités avec des patchs à micro-aiguilles, carrés d'une surface de 1,5 cm2, contenant 86 micro-aiguilles et ayant 450 ± 23,5 µm de hauteur avec 1 mm d'espacement entre les micro-aiguilles. Un traitement histologique et des colorations ont été réalisée pour observer la viabilité cellulaire et les glycosaminoglycanes. La diffusion de FITC a été observée en épifluorescence. Le pourcentage de surface colorée pour chaque traitement a été comparé à des échantillons témoins non traités à différents temps de cinétique. Un test de Mann-Whitney a été utilisé pour identifier la différence entre deux populations (sites de pénétration des micro-aiguilles et peau normale) avec une limite de significativité statistique de $p < 0,05$.

RÉSULTATS: L'application du patch MN sur les explants de peau a montré que ces micro-aiguilles ne pénétraient dans le derme de la peau. L'application cutanée des patchs MN a révélé 17 sites différents de pénétration de micro-aiguille immédiatement après l'application et 4 sites, 2 heures plus tard. Bien qu'il y ait eu quelques variations dans la profondeur de pénétration épidermique, ces variations n'ont pas eu d'impact sur la viabilité cellulaire. Les micro-aiguilles à base d'acide hyaluronique d'une longueur de 450 µm ont pénétré l'épiderme à une profondeur moyenne de 26 µm sans perturber la viabilité des cellules de la peau et sans provoquer de réponse inflammatoire. L'acide hyaluronique composant les micro-aiguilles a été détecté sur la plupart

de ces sites de pénétration, sans diffusion dans le derme, ce qui est important pour les applications cosmétiques. L'analyse FTIC a révélé une distribution d'isothiocyanate de fluorescéine dans le site d'insertion de micro-aiguille qui est restée stable après 2 et 6 heures d'expérimentation.

CONCLUSIONS: En utilisant des études de coloration de traceurs sur explant de peau humaine ex vivo, nous avons montré que l'applicateur de micro-aiguille est capable de pénétrer l'épiderme et de délivrer des substances incorporées dans la matrice polymère de l'aiguille. De plus, le produit testé s'est avéré sûr et bien toléré, ce qui ouvre une large perspective pour l'administration d'agents cosmétiques et pharmaceutiques.

Introduction

Non-invasive methods of skin delivery are the subject of much research and development, yet controlling effective delivery is difficult. As a route for both cosmetic and drug permeation, the skin is very attractive for scientists, yet presents a notable challenge due to its unique structural design as a barrier to the external environment. Furthermore the skin changes with time — chronologically and environmentally (UV, diet, pollution, etc). In addition, various skin conditions which can also fluctuate with time as well as both external and internal environments, such as atopic dermatitis, acne, etc., add to these challenges.

For the improvement of ageing parameters, especially wrinkle deformations, effective delivery of actives is a real consumer desire. In the aesthetic field of cosmetic treatments the interest in micro-needle technology (MN) in the form of applied skin patches, originally developed for drugs, continues to grow. As a physical method of skin delivery, MN devices dramatically increase the permeation of 'actives' across the stratum corneum [1,2].This type of delivery technology for cosmetic use presents a number of challenges as well. Firstly, it is invasive, and controlling the needle size is paramount especially for cosmetics. Also needles were originally made from steel and silica presenting safety issues [3,4]. Furthermore, the actual needle size also has to take into consideration changes in skin depth which changes with both age and body site.

We have developed and patented a MN patch based on soluble micro-needles [5] . Literature studies have confirmed the histological and clinical effects of micro-needle treatments of scars, stretch marks, wrinkles, and facial rejuvenation using the Dermaroller and analogs with stainless steel 1-1.5 mm needles [6-8]. Moreover, recent studies have shown the effectiveness of applicators with an area of 100 - 200 mm2, containing 49 soluble conical micro-needles with a height of 220-250 microns, and loaded with sodium hyaluronate and other active components such as adenosine, retinyl retinoate, ascorbic acid and horse oil [9-12].

The benefits of using dissolvable micro-needle patches with hyaluronic acid for bio-revitalisation and collagen-induction therapy in the periorbital area are painlessness, noninvasiveness, controlled following of the predetermined depth of injection, ease of use and a short rehabilitation period after the procedure due to the absence of damage to capillaries and nerve endings [13,14]. Dissolving micro-needles are fabricated with biodegradable polymers by encapsulating the drug into the polymer. After inserting the micro-needle into the skin, dissolution takes place which releases the active. Unlike other micro-needles, the application involves only a single step as the micro-needle is soluble. Effective distribution is an important factor which faces problems while developing dissolving micro-needles. Hence, polymer-active mixing is a critical step in such fabrication [15,16].

In our studies, we evaluated the effectiveness of a patch applicator containing 650 micro-needles. To overcome skin deformation that (due to the viscoelasticity of the skin) occurs when such needles are inserted and to ensure effective penetration of the skin, conical micro-needles increased in height to 450±23.5 microns were used [17]. Since the MN patch we have developed is designed for the periorbital area of the face, high efficiency of dissolvable hyaluronic micro-needles in correcting involutional changes of the periorbital area is a key expectation and requirement [18,19]. In a following paper [20], we report the clinical safety and efficacy of these soluble MN patches, which comprise 650 micro-needles containing hyaluronic and ferulic acids.

The aim of the paper presented herein is the description and safety evaluation of the
process of dissolution of an 86 micro-needle MN patch composed of hyaluronic acid, when applied topically to human abdominal skin explants. Such explants were chosen to replace the inability of obtaining periorbital skin. In order to evaluate penetration and dissolution of the micro-needles we employed histochemical methods and a fluorescent dye FITC (fluorescein isothiocyanate).

Visualisation of a cell with fluorescent tracer compounds provides a wide variety of information for the analysis of cell functions [21] . Various activities and structures of a cell can be targeted for staining with fluorescent compounds [22]. The most commonly stained cell components are cell membranes, proteins, and nucleotides. Small neutral molecules and positively charged molecules can pass through viable cell membranes and remain inside of cells, depending on their reactivity or hydrophilicity. Negatively charged molecules cannot pass through viable cell membranes. Positively charged molecules are usually cell membrane permeable and accumulate in the mitochondria. The ester functional group is suitable for staining viable cells because it can pass through viable cell membranes, where it is hydrolysed by cellular esterases into a negatively charged molecule under physiological conditions. Several fluorescein analogs with ester groups in their structure are available for viable cell staining. Succinimidyl ester compounds can also be used to improve the retention of the fluorescent derivative within the cell [23]. These compounds are neutral molecules that pass-through cell membranes and covalently conjugate with cell

proteins. Covalently-conjugated molecules can stay in the cell for several weeks.

Materials and methods

Explant preparation

On day 0, an abdominoplasty (Female, Caucasian, 44 years) was stripped 5 times using Scotch 3M adhesive tape, and 3 excised skin bands of 13 cm x 5 cm were delimited for the MN patch application. 36 explants of an average diameter of 12 mm (±1mm) were prepared and placed in survival in BEM culture medium (BIO-EC's Explants Medium) at 37℃ in a humid, 5 %-CO2 atmosphere. Explants were distributed in two batches of 18 explants, one untreated control and a batch treated with test product.

Test Product

The test product comprised micro-needle patches based on dissolving, detachable micro-needle technology (Russian Federation patent for invention No. 2652567 "Microneedle patch and the way of it's manufacturing"; US patent "A micro-needle patch for transdermal injections" EFS ID: 32735812, WO/2019/231360) were produced by Microneedle Industrial LLC (Moscow, Russia).

In order to evaluate micro-needle penetration and their dissolution capabilities, square micro-needle patches with a 1,5 cm^2 surface area, containing 86 micro-needles and having 450±23,5 µm in height with 1 mm interspacing between nearest neighbouring micro-needles, were fabricated. The foregoing

dimensional characteristics were followed in accordance with BIO-EC specifications, aiming to provide a reasonable convenience of micro-needles patches application onto ex vivo skin explants (36 explants of an average diameter of 12±1 mm).

Briefly, the fabrication process was conducted with needle-shape micro-molds using hyaluronic acid (average Mw = 0.4x106; Xian Lyphar Biotech Co. Ltd., China) as the base material. The hyaluronic acid (HA) solution was prepared in distilled water containing 2.5% (w/w) HA and 0,05% (w/w) maltose (Sigma-Aldrich, USA). The additives for skin improvement were mixed with the HA solution and the final concentration of ferulic acid (Sigma-Aldrich, USA) was 0,10% (w/w). The resulting solution was cast onto the micro-mold and dried at 45ºC in a desiccator. After 6 hours of drying, the adhesive film was attached to the base plate and the combined microneedle patch was obtained by peeling off the mold (Fig.1)

For the estimation of FITC marker distribution, a supplementary batch of micro-needle applicators was fabricated as described with the addition of fluorescein isothiocyanate taken in a concentration of 0,01% w/w.

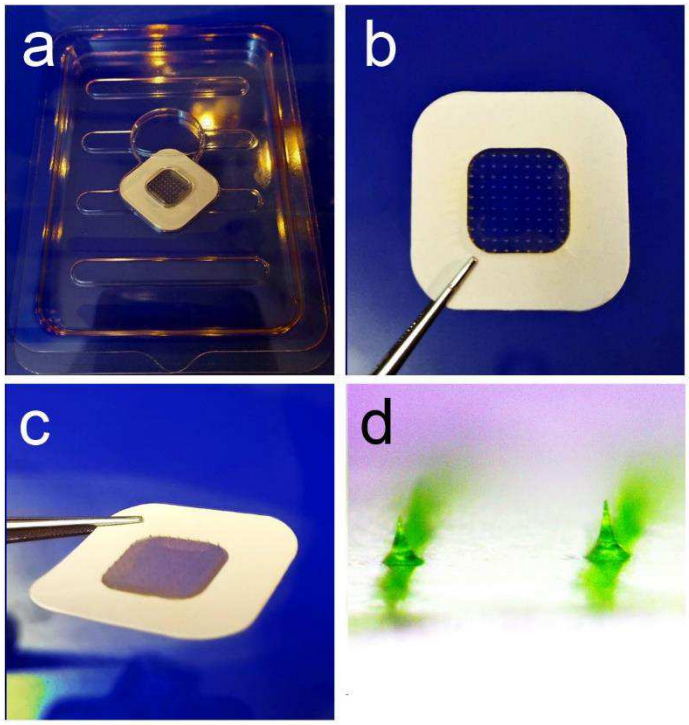

Figure 1: Fabrication of micro-needle patches: Micro-needle patch (a), Square micro-needle patch with 1,5 cm^2 surface area (b), Square micro-needle patch containing 86 micro-needles (c), Micro-needles with FITC marker (d)

Product application

On day 0, the MN patches (P) were applied onto the excised skin bands of 13cm x 5 cm with a homogeneous pressure of 225g/cm2 for 40 minutes using loads. Patch application was prolonged without the loads one additional supplementary hour. The same pressure was applied to the untreated batch (T) without patch for 40 minutes with loads, followed by 1 hour without loads. The culture medium was half renewed (1 ml per well) on days 1 and 4 respectively.

Sampling and h**istological processing**

On day 0, immediately at the end of the application time, 3 explants from the batch T0 and P0 were collected and cut into two parts. Half were fixed in buffered formalin solution and the other half were frozen at -80℃. On day 0+2h (2h after the end of patch application), day 0+6h (6h after the end of patch application), day 1 (24h after the end of patch application), day 2 and day 5, 3 explants from each batch were collected and processed in an identical manner to those explants described for day 0. After fixation for 24 hours in buffered formalin, skin samples were dehydrated and impregnated in paraffin using a Leica PEARL dehydration automat, and then embedded using a Leica EG 1160 embedding station. 5-µm-thick serial sections were made using a Leica RM 2125 Minot-type microtome, and the sections were mounted on Superfrost® histological glass slides. Skin samples which had been frozen were cut to 7-µm thickness with a Leica CM 3050 cryostat. The serial sections were then mounted on silanised glass slides Superfrost® Plus. Microscopic observations were realised with a Leica DMLB or Olympus BX43 microscope and images digitised with a numeric DP72 Olympus camera with CellD storing software.

Cell viability

Cell viability of both epidermal and dermal structures were assessed by microscopic observation of the paraffin sections following Masson's trichrome staining, Goldner variant [24] . Stained samples (T and P on day 0 (immediate and 2h), day 2 and day 5 (24 explants) were then assessed by microscopic observation and image analysis.

Distribution of FITC marker

The distribution of the fluorescent dye FITC (fluorescein isothiocyanate) across the various layers of the skin (frozen skin sections) was evaluated by microscopic observation in epifluorescence and image analysis. Image analysis of the distributed FITC marker was performed on the site of micro-needle injection, and skin areas around 500-600 µm away from the injected site. Samples examined were taken from explants T and P on day 0 (immediate, 2h and 6h).

Acidic Glycosaminoglycan (GAGs) staining

Since the basic composition of the MN patch is composed of hyaluronic acid (HA), dissolution of the micro-needles within the skin at different time points was visualised by Alcian Blue staining of acidic glycosaminoglycans, which includes hyaluronic acid. Staining was assessed by microscopic observation of skin samples T and P on days 0 (immediate and 2h), 2 and 5.

Image analysis

For all batches of explants, the percentage of the region of interest covered by staining

(stained surface percentage) was determined by image analysis using using the image analysis module of the Olympus CellD software. The stained surface percentage for each treatment was compared to untreated samples (P versus T) at the given time points. Mann-Whitney Test was used to identify the difference between two populations (sites of skin samples punctured with

stained and clear micro-needles respectively) at the given level of statistical significance ($p<0.05$).

Results

Cell viability - Cell viability was well maintained throughout the course of the investigation. On Day 0, immediate observations revealed good cell viability in both the epidermis and dermis. Cell viability assessed immediately after the MN patch application also showed good viability with no modification induced by the patch (Fig. 2a).

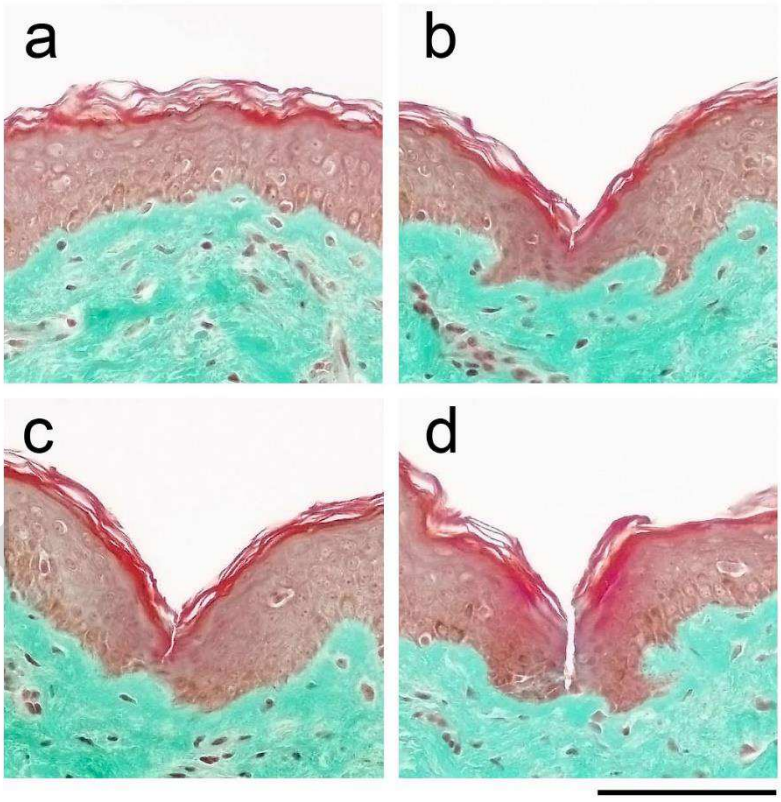

Figure 2: Masson's trichrome staining immediately after application of the patch (P0) showing normal skin between needles (a), penetration site through stratum corneum (b), penetration site through epidermis (c), penetration site reaching dermal-epidermal junction (d). Scale bar = 100µm.

Immediately after application of the patch (P0), seventeen different sites of micro-needle penetration were identified: 1 site passed through the stratum corneum only (Fig. 2b); 7 sites partially passing through the epidermis without reaching the dermal-epidermal junction (Fig. 2c); and 9 sites completely passing through the epidermis reaching the dermal-epidermal junction (Fig. 2d) . There was no penetration of the papillary dermis.

Two hours post-patch application (P0+2h), 4 different sites of micro-needle penetration were identified: 1 site passing through the stratum corneum only; 1 site partially passing through the epidermis without reaching the dermal-epidermal junction; 1 site completely passing through the epidermis reaching the dermal epidermal junction; and 1 site passing through the papillary dermis (Fig. 3).

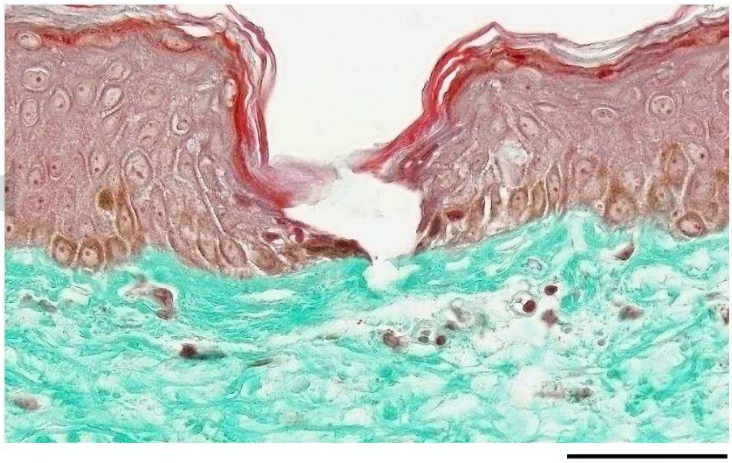

Figure 3: Masson's trichrome staining 2 hours after after application of the patch (P0+2h) on showing the only penetration site through the papillary dermis. Scale bar = 50 µm.

On Days 2 and 5, cell viability of the untreated skin samples was fairly good in dermis and good in the dermis. When the patch was applied, no modification in cell viability was observed.

Micro-needle penetration through the skin (P0 and P0+2 hours) was also measured (Fig. 4a).

	Microneedles penetration depth (µm)	
	P0	**P0+2h**
Average	**25,9**	**22,1**
SD	11,8	10,9

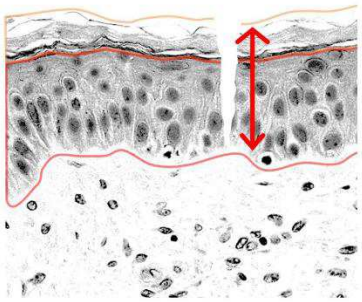

Figure 4a: Histochemical illustration of the micro-needle penetration into the skin.

On Day 0, immediately after patch application (P0), the average penetration depth of the micro-needles was 25,9 µm, and at 2 hours post application, the penetration of the micro-needles was reduced to 22,1 µm. However, there was no significant difference between the penetration depth of the micro-needles comparing these two time points (Fig. 4b).

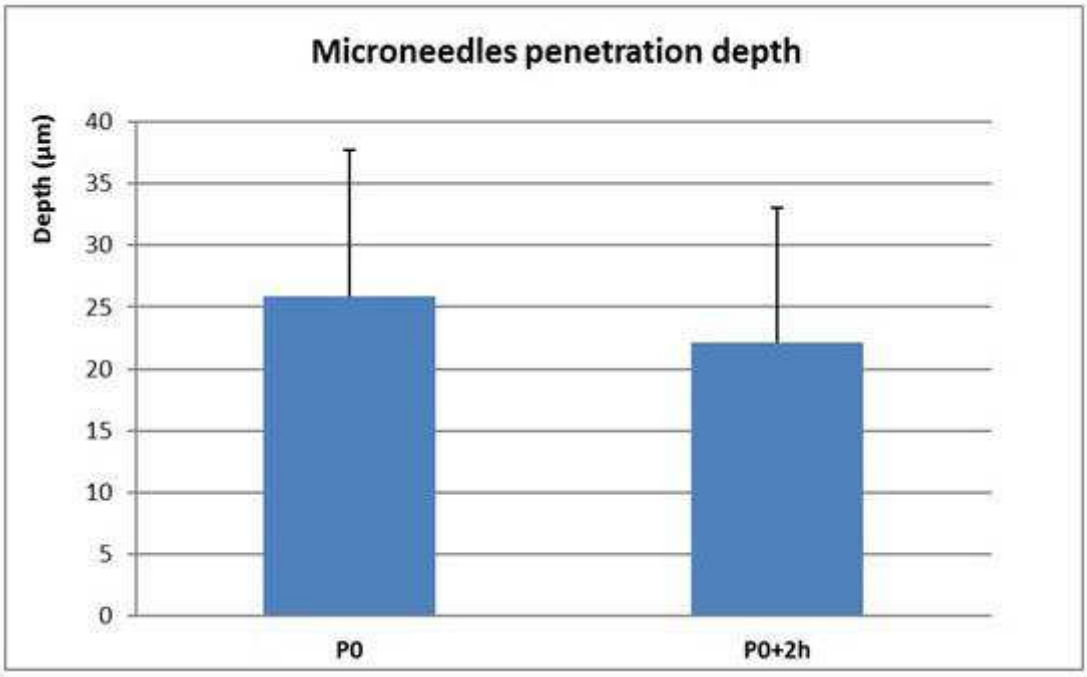

Figure 4b: Comparison of micro-needles penetration immediately after application as compared to 2 hours post application.

FITC distribution - The average epidermal penetration of FITC was analysed on the site of injection, and on the normal zone 500-6000 µm from the site of injection (Fig. 5a). No fluorescent signal was observed on the control (T0) batch. The surface percentage occupied by FITC in the epidermis of the other batch is shown in Fig. 5b.

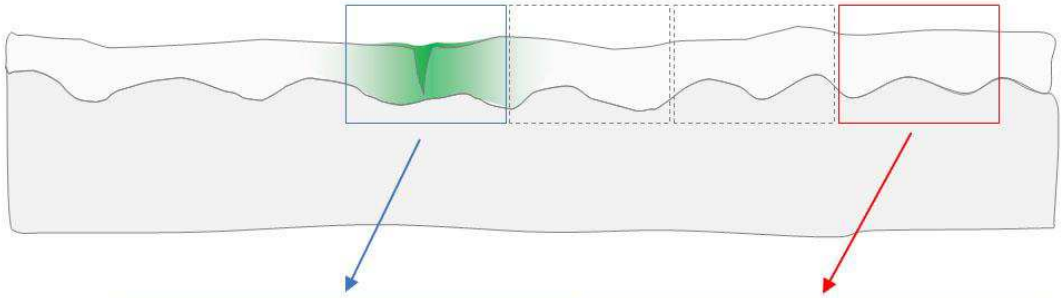

	FITC penetration in the site of injection (% surface)			FITC penetration in normal zone (% surface)		
	P0	P0+2h	P0+6h	P0	P0+2h	P0+6h
Average	**71,3**	**77,9**	**71,8**	**42.4**	**49.9**	**39.4**
SD	20,2	17,4	22,1	32.1	30.4	27.4

Figure 5a: Comparative measurement of FITC penetration on injection site and normal zones (under patch between injection sites), immediately and 2 hours and 6 hours following MN patch application.

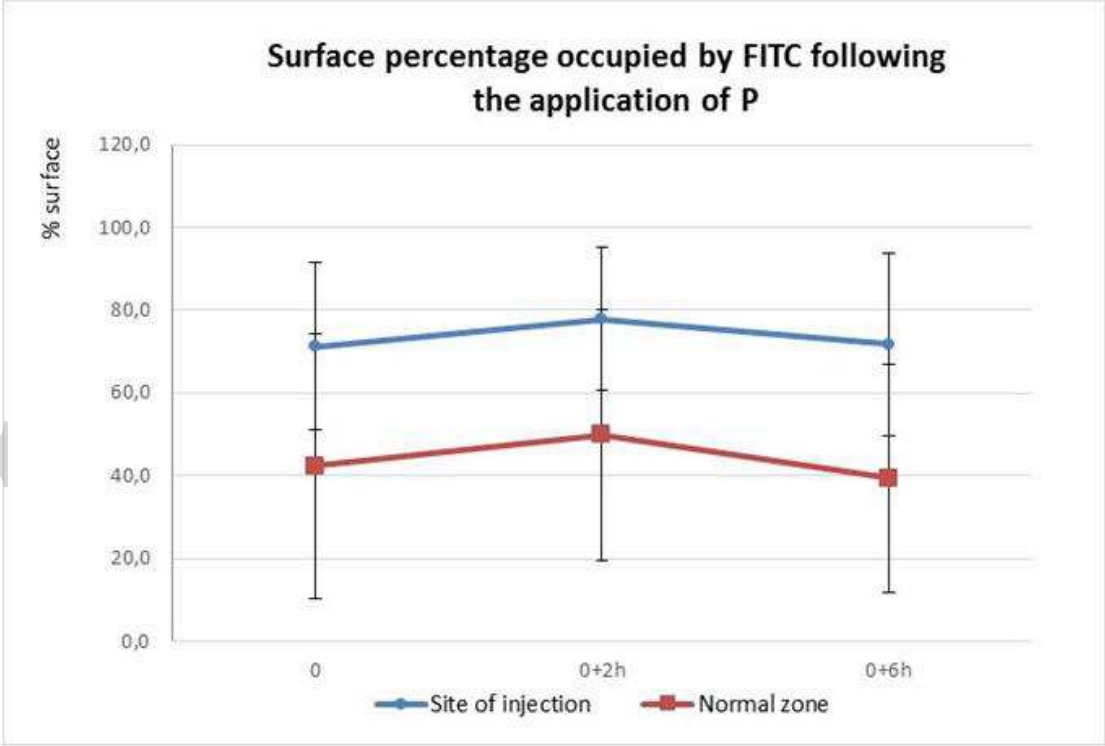

Figure 5b: Kinetic of FITC diffusion into the epidermis on injection site and normal zones (under patch between injection sites) within 6 hours following MN patch application.

At the injection site on Day 0, and immediately following application (P0), the test product (P) the surface percentage occupied by FITC within the epidermis was 71.3%. Furthermore, 6 hours post-application (P0+6h), the surface percentage occupied by FITC was non-significantly increased by 1%. At the Normal Zone (500_600 µm from the site of injection), on Day 0, and immediately following application (P0), the surface percentage occupied by FITC in the epidermis was 42.4%. Comparing with P0, 2 hours after application (P0+2h), the surface percentage occupied by FITC was non-significantly increased by 18%. 6 hours after application (P0+6h), the surface percentage occupied by FITC was non-significantly decreased by 7% (Figure 5c).

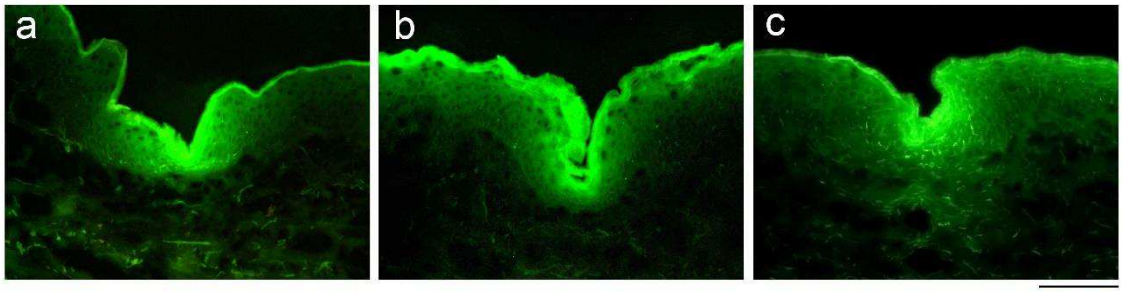

Figure 5c: FITC diffusion immediately after patch application (a), 2 hours later (b) and 6 hours (c) later. Scale bar = 100µm.

Acidic Glycosaminoglycans (GAGs) staining - No staining of acidic glycosaminoglycans (GAGs) was observed in the epidermis of the different batches. The acidic GAGs (including hyaluronic acid) in the papillary dermis of the different batches is shown in Fig. 6

On Day 0, the content of acidic GAGs in the untreated control (T0) was observed fairly clearly in the papillary dermis. Immediately following MN patch application the effect on the content of acidic GAGs as compared to the control (T0) showed that the patch induced no modification (Fig. 6a).

With the product patch P, immediately after application (P0), 16 different sites of micro-needles (out of 17) exhibited intense acidic GAGs staining. Hyaluronic acid was observed at the surface of the penetration site (stratum corneum and/or epidermis) without any diffusion into the epidermis or dermis. Image analysis was not performed since the staining was localised to the surface of the epidermis and stratum corneum without any diffusion into the epidermal cell layers (Fig. 6b)

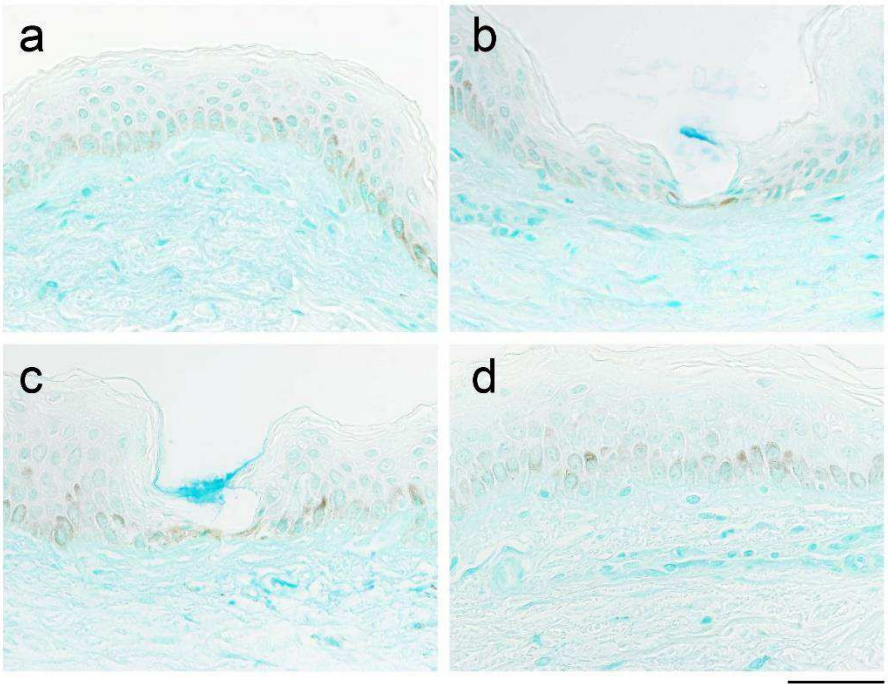

Figure 6: Glycosaminoglycan staining of injected site (a) at T0; (b) immediately after injection P0; (c) 2 hours post injection showing intense staining at entry site (P0+2h); and (d) with no modification. Scale bar = 50µm.

On Day 0+2h, the content of acidic GAGs in the control (T0+2h) was moderate to fairly clear within the papillary dermis. Following MN patch treatment, 2 hours post-application, and comparing to T0+2h a slight decrease in staining was observed .Two hours post-application (P0+2h), 3 different sites of micro-needles (out of a total of 4) exhibited intense hyaluronic acid staining. Hyaluronic acid was observed at the surface of the penetration site (stratum corneum and/or epidermis) without any diffusion into the epidermis or dermis (Fig. 6c) . On Day 2 , the control samples , the content of acidic GAGs was observed as weak in the papillary dermis. Two days post-application of the MN

patch the content of acidic GAGs, as compared to the control Day 2 showed that the product induced no modification in staining intensity. On Day 5, the control samples, the content of acidic GAGs was observed as weak in the papillary dermis. Post-application of the MN patch did not modify these observations (Fig 6d).

Discussion

The application of the MN patch to excised skin explants illustrated our micro-needles to be non-invasive into the dermis of the skin which potentiates their use for cosmetic applications. MN tips were sharp enough to breach the stratum corneum as evident from Figures 1 and 2. The primary principle of the MN patch involves disruption of the skin layer, thus creating micron size pathways that lead the actives directly to the epidermis. Our newer form of micro-needles helps to enhance the delivery of actives through the skin overcoming the various problems associated with conventional topical formulations.

As might be expected, skin puncturing with MN patches revealed 17 different sites of micro-needle penetration immediately afterwards and 4 sites, 2 hours later. We have also shown that while there are some variances in the epidermal depth of penetration, these variances did not impact on cell viability. Although we did not histologically mark for an inflammatory response, this was a given since micro-needles will cause some minor irritation at the point of entry, and we observed this in our clinical findings as reported in the following paper [20]. Hyaluronic acid could be detected in most of these penetration sites, with no diffusion into the dermis., which is important for cosmetic applications. The

current study clearly demonstrates that hyaluronic acid-based micro-needles having 450 µm in length penetrate epidermis at a length of averagely 25 µm without disrupting skin cells viability and without causing inflammatory response. From this perspective, micro-needle length and the corresponding intrinsic penetration depth appear to be non-identical (in the case of using polymer micro-needle patches), and is dependant on various factors including micro-needle polymer composition, stiffness, micro-needle shape parameters, etc. The obtained data indicate that either measuring intrinsic micro-needle penetration depth based on the length of needles or evaluating micro-needles mass loss after the insertion into skin, is generally not enough to gain valid results as we have shown. Moreover, it is necessary to formulate additional methods of safety assessment of either micro-needle patches or analogous products, which are not currently provided by ISO 10993-1 «Biological evaluation of medical devices Part 1: Evaluation and testing within a risk management process» [25]

Regarding acidic glycosaminoglycans (GAG) analysis which did not uncover any significant GAG concentration changes before and after micro-needle insertion, it is worth noting that micro-needles were manufactured with hyaluronic acid having a relatively small molecular weight (~400 kDa) which undergoes rapid disintegration by skin enzymes. Probably, more sensitive and/or rapid analysis approaches should be carried out for successful performance of residual GAG estimation in skin explants containing living cells to counter-balance the occurring molecules cleavage. Despite the absence of

significant changes of GAG concentration, FTIC analysis uncovered fluorescein isothiocyanate distribution within the micro-needle insertion site and its characteristics remained steady after 2 and 6 hours of experimentation.

Conclusions

Using ex-vivo tracer staining studies, we have shown that the evaluated micro-needle applicator is capable of penetrating the skins epidermis and deliver substances embedded in the needle polymer matrix. In addition, the tested product was proven safe, which provides for a broad perspective for delivering cosmetic and pharmaceutic agents. In a following paper we describe the clinical and efficacy and safety evaluation of these micro-needle patches.

Acknowledgement

The authors would like to thank Dr Theresa Callaghan, Callaghan Consulting International Hamburg, Germany for the preparation of this manuscript. Final editing was executed by the authors.

Conflict of interest

The authors declare no conflict of interest. Work was fully funded by Microneedle Industrial LLC and Laboratoire BIO-EC

References

1. Akhtar, N. Microneedles : An Innovative Approach to Transdermal Delivery - A Review. Int. J. Pharm. Pharm. Sci. **6**,18–25 (2014)

2. Bariya, S.H., Gohel, M.C., Mehta, T.A., & Sharma, O. P. Microneedles: an emerging transdermal drug delivery system. J. of Pharm. Pharmacol. **64,** 11–29 (2012)

3. Ita K. Transdermal delivery of drugs with microneedles - potential and challenges. Pharmaceutics **7,** 90–105 (2015)

4. Donnelly R., Singh T., Woolfson A. Microneedle-based drug delivery systems:
microfabrication, drug delivery, and safety, Drug Deliv. **17**, 187-2017 (2010)

5. Zvezdin V., Akafeva T., Kasatkin I. A Microneedle patch for transdermal injections.
Pub. No.:WO/2019/231360, 28.05.2018 US.
https://patentscope.wipo.int/search/en/detail.jsf?docId=WO2019231360&_cid=P21-K4LA6D-58196-1

6. Horst, L., Luther, C. K. Skin cell proliferation stimulated by microneedles. J. Am. Coll. Clin. Wound Spec. **4,** 2-6 (2013)

7. Satish, D. Microneedling with Dermaroller. J. Cutan. Aesthet. Surg. **2**, 110–111 (2009)

8. Majid I. Microneedling therapy in atrophic facial scars: An Objective Assessment. J. Cutan. Aesthet. Surg. **2**, 26–30 (2009)

9. Choi, SY., Kwon, HJ., Ahn, GR., et al. Hyaluronic acid microneedle patch for the improvement of crow's feet wrinkles. Dermatol. Ther. **30**, e12546 (2017)

10. Kang, G., Tu, T.N.T., Kim, S., Yang H., Jang M., et al. Adenosine-loaded dissolving microneedle patches to improve skin wrinkles, dermal density, elasticity and hydration. Int. J Cosm. Sci. **40**, 199-206 (2018)

11. Kim, M., Yang, H., Kim, H., Jung, H., Jung, H. Novel cosmetic patches for wrinkle improvement: retinyl retinoate- and ascorbic acid-loaded dissolving microneedles. Int. J. Cosm. Sci. **36**, 207-212 (2014)

12. Lee, C., Eom, Y.A., Yang, H., Jang, M., Jung S.U., et al. Skin barrier restoration and
moisturization using horse oil-loaded dissolving microneedle patches. Skin Pharmacol. Physiol., **31**, 163-171 (2018)

13. Iriarte, C. Awosika, O., Rengifo-Pardo, M., Ehrlich, A. Review of applications of microneedling in dermatology. Clin. Cosm. Invest. Dermatol, **10**, 289–298

(2017)

14. Mero, A.,Campisi, M. Hyaluronic acid bioconjugates for the delivery of bioactive molecules. Polymers, **6**, 346–369 (2014)

15. Prausnitz, M. Engineering microneedle patches for vaccination and drug delivery to skin, Annu. Rev. Chem. Biomol. Eng. **8,** 177–200 (2017)

16. Waghulea T., Singhvia G., Dubeya S., Pandeya M., Guptab G., Singh M., Duac K. Microneedles: A smart approach and increasing potential for transdermal drug delivery system. Biomedicine & Pharmacotherapy **109**,1249-1258 (2019)

17. Martanto, W., Moore, J.S., Couse, T., Prausnitz, M.R. Mechanism of fluid infusion during microneedle insertion and retraction. J. Control. Rel. **112**, 357–361 (2006)

18. Choi, S.Y., Kwon, H.J., Ahn, G.R., et al. Hyaluronic acid microneedle patch for the improvement of crow's feet wrinkles. Dermatol. Therapy, **30**, 1–5 (2017)

19. Yang, J.A., Kim, E.S., Kwon, J.H., Kim, H., et al. Transdermal delivery of hyaluronic acid - Human growth hormone conjugate. Biomaterials, **33**, 5947–5954 (2012)

20. Zvezdin V., Kasatkina T., Kasatkin I., Gavrilova M., Kazakova O. Microneedle patch
based on dissolving, detachable microneedle technology for improved skin quality of the
periorbital region. Part 2: Clinical evaluation Int. J. Cosm. Sci (2020) submitted.

21. Hermanson G., Fluorescent Probes, in Bioconjugate Techniques (Third Edition), 2013 https://doi.org/10.1016/C2009-0-64240-9 Academic Press, Elsevier (2013)

22. Beutner E., Holborow E., Johnson G. Quantitative studies of immunofluorescent staining. I. Analyses of mixed immunofluorescence. Immunology, **12**, 327-37 (1967)

23. Beem E., Segal M. Evaluation of stability and sensitivity of cell fluorescent labels when used for cell migration. J Fluoresc. **23**, 975-87 (2013)

24. Goldner J. A modification of the Masson trichome techniques for routine laboratory purposes. Amer. J. Pathol. **14**, 237-243 (1938)

25. ISO 10993-1:2018 Biological evaluation of medical devices — Part 1: Evaluation and testing within a risk management process. https://www.iso.org/standard/68936.html